

Genome Mining Guided Discovery of Macrocyclic Sesterterpenoids with Anti-MRSA and Anti-Neuroinflammatory Activities

Keying Lan, Zhennan Wang, Kangjie Lv, Cuiping Xing, Xiaoying Li, Qiang Yin, Yuwei Chen, Xuming Mo, Xiaobo Mao, Weijie Wu, Tom Hsiang, Lixin Zhang, Huanqin Dai, Xueting Liu, Guoliang Zhu,* and Lan Jiang*



Cite This: *J. Agric. Food Chem.* 2025, 73, 32674–32684



Read Online

ACCESS |



Metrics & More



Article Recommendations



Supporting Information

ABSTRACT: Terpenoids exhibit antioxidant, antimicrobial, and health-promoting activities, and are widely utilized in the food industry. In this study, a new bifunctional terpene synthase (BFTPS) and its associated gene cluster were identified in *Colletotrichum cereale* 00173 through a genome mining approach. Heterologous expression of the BFTPS and its gene cluster in *Aspergillus oryzae* NSAR1 led to the production of a 14-membered macrocyclic sesterterpene, colcerepene (**1**), and four hydroxylated derivatives, colcerepenoids A–D (**2–5**). The biosynthetic pathway of compounds **1–5** was further elucidated through feeding experiments. Notably, compound **1** exhibited antibacterial activity against methicillin-resistant *Staphylococcus aureus* (MRSA) with an MIC value of 6.25 μ M. This study is the first report of *anti*-MRSA activity in macrocyclic sesterterpenoids, expanding the functional space of macrocyclic sesterterpenoids as promising leads for developing agents against foodborne pathogens.

KEYWORDS: bifunctional terpene synthases, macrocyclic sesterterpenoids, heterologous expression, biosynthetic pathway, antibacterial activity

INTRODUCTION

The escalating global burden of antimicrobial resistance (AMR) poses severe threats to food security and public health, with pathogens like methicillin-resistant *Staphylococcus aureus* (MRSA) complicating the treatment of foodborne infections and diminishing the efficacy of agricultural antibiotics.^{1–3} MRSA is a multidrug-resistant pathogen that can contaminate food during processing or handling via infected or asymptomatic carriers.^{4,5} Insufficient cooking or improper storage conditions may enable its survival, leading to ingestion, intestinal colonization, and in some cases, secondary infections.⁶ Although current treatments such as vancomycin and linezolid are effective, their use is limited by cost, toxicity, and resistance development.⁷ Therefore, there is an urgent need for novel and safe antimicrobial agents that can overcome existing resistance mechanisms.

Macrocyclic terpenoids defined by carbon rings of 12 or more members, are considered biosynthetic precursors to more complex polycyclic terpenoids.⁸ Their constrained ring systems and diverse functional groups often lead to enhanced target selectivity.^{9,10} For example, cembranoids, primarily present in marine coelenterates and higher plants, possess a 14-membered carbon ring and demonstrate significant cytotoxic, anti-inflammatory, and antimicrobial activities.¹¹ Additionally, the 18-membered macrocyclic sesterterpenoids cyclooctadecatetraene and the 14-membered cericerene, derived from plants, exhibit notable immunosuppressive activity.¹²

Fungi represent a promising resource for structurally complex scaffolds exhibiting potent bioactivities, and terpenoids represent one of their most diverse and pharmacologically significant compound classes.^{13–16} However, a key

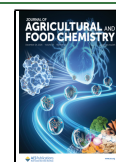
bottleneck in harnessing fungal terpenoids lies in their low natural abundance and the cryptic nature of their biosynthetic pathway. While bacteria and plants typically utilize separate prenyltransferases (PTs) and terpene cyclases (TCs) for terpenoid biosynthesis, filamentous fungi encode a single bifunctional terpene synthase (BFTPS), which integrates a TC domain at the N-terminus and a PT domain at the C-terminus. The TC domain contains the conserved DDXXD(E) and NSE motifs, while the PT domain features a single conserved DDXXD motif. This bifunctional enzyme efficiently catalyzes both the chain elongation of isoprene units and the subsequent cyclization, enabling streamlined terpenoid scaffold formation.¹⁷ These initial scaffolds are further modified by tailoring enzymes to produce a wide variety of terpenoid compounds.^{18,19} Despite this, the enzymes responsible for synthesizing macrocyclic terpenoids in microorganisms remain largely uncharacterized. To date, only one fungal macrocycle-producing BFTPS, CgCS from *Colletotrichum gloeosporioides* has been reported.²⁰ Advances in genome mining and heterologous expression now enable targeted activation of these cryptic pathways,^{21,22} while feature-based molecular networking (FBMN) accelerates the identification of trace derivatives through MS/MS pattern recognition.^{23,24}

Received: August 29, 2025

Revised: November 7, 2025

Accepted: December 5, 2025

Published: December 14, 2025



In this study, we identified CcMS, the first natural fungal BFTPS from *C. cereale* 00173 functionally characterized to catalyze the synthesis of a macrocyclic sesterterpene scaffold. Heterologous expression of the associated biosynthetic gene cluster in *Aspergillus oryzae* led to the characterization of a 14-membered macrocyclic sesterterpene, colcerepene (**1**), along with four new sesterterpenoids (**2–5**) derived from **1** with different hydroxyl substitutions. Critically, compound **1** exhibited potent activity against MRSA (MIC = 6.25 μ M), while derivatives **2–5** showed selective antineuroinflammatory activity in BV2 microglia. The biosynthetic pathway of these compounds was also proposed based on feeding experiments. This work demonstrates how integrated genomics and metabolomics can unlock fungal terpenoid diversity for biomedicine and food safety applications, providing a sustainable platform for antimicrobial discovery.

MATERIALS AND METHODS

Chemical Experimental Materials. NMR, HR-ESI-MS, LC-HRMS (ESI), RP-HPLC, and GC-MS analyses were performed as described previously.^{22,25} CD spectra were recorded on a Chirascan circular dichroism spectrometer using acetonitrile as solvent. Optical rotation was measured with either a Rudolph Research Analytical Autopol V Automatic Polarimeter or a JASCO P-2200 digital polarimeter. Biological reagents, chemicals, and media were sourced from standard commercial suppliers unless otherwise noted.

Bioinformatics Analysis. Multiple sequence alignments were generated with ClustalW. A phylogenetic tree was constructed using the maximum likelihood algorithm implemented in MEGA X software (v. 10.2.6) with 1000 bootstrap replicates.²⁶ The tree was subsequently visualized and refined using the iTOL software (v. 7.2.2) (<https://itol.embl.de/>). The candidate gene CcMS was retrieved from our in-house genome database.

Strains and Media. *C. cereale* 00173 (CGMCC 40894) was isolated from *Agrostis stolonifera* near Toronto, Canada. It was cultivated on 2% potato dextrose agar (containing potato extract 0.4%, glucose 2%, agar 2%) at 28 °C for 3–5 days for gene cloning. All cloning procedures were conducted using *Escherichia coli* DH10B. The strain *A. oryzae* NSAR1 (*niaD*[−]*sC*[−]*adeA*[−] Δ *argB::adeA*[−]),²⁷ was utilized as the host for heterologous expression. This host was initially grown in DPY broth, and the resulting transformants were subsequently cultured in MPY broth. The specific compositions of both media and the detailed cultivation protocols have been described in our previous work.^{22,25}

Transformation of *A. oryzae*. Genomic DNA of *C. cereale* 00173 was extracted following the previously reported method.²² Genes included in the *col* biosynthetic gene cluster (*orfA*, *colB*, *colC*, and *colD*) were amplified using Q5 High-Fidelity Polymerase (NEB), with the genomic DNA serving as the template (Table S1). The PCR products were cloned into pUARA4 or pUSA4, the constructed plasmids are listed in Table S2.

A. oryzae NSAR1 protoplasts were prepared following the protoplast-polyethylene glycol method reported previously,²⁸ and the following transformants were constructed (Table S3): AO-*colD* (pUARA4-*colD*), AO-*orfA/colBCD* (pUARA4-*colD* and pUSA4-*orfA/colBC*), AO-*orfA* (pUSA4-*orfA*), AO-*colB* (pUSA4-*colB*), AO-*colC* (pUSA4-*colC*), AO-*orfA/colD* (pUARA4-*colD* and pUSA4-*orfA*), AO-*colBD* (pUARA4-*colD* and pUSA4-*colB*), AO-*colCD* (pUARA4-*colD* and pUSA4-*colC*), AO-*orfA/colBD* (pUARA4-*colD* and pUSA4-*orfA/colB*), AO-*orfA/colCD* (pUARA4-*colD* and pUSA4-*orfA/colC*) and AO-*colBCD* (pUARA4-*colD* and pUSA4-*colBC*). The nomenclature for the transformants follows the format of the host, followed by the transformed gene(s).

Analysis of Metabolites of BFTPS Transformant. To prepare the seed culture, BFTPS transformant AO-*colD* was seeded into 100 mL of MPY medium within 250 mL Erlenmeyer flasks. The fermentation was then scaled up, using 1000 mL of the same medium in 3000 mL flasks. Mycelia of the BFTPS transformant AO-*colD* were

inoculated into 250 mL Erlenmeyer flasks containing 100 mL of MPY medium to prepare the seed culture. Fermentation was carried out in 3000 mL flasks with 1000 mL of MPY medium. A cell pellet (0.5 kg) was obtained by filtering the culture broth (10 L) of AO-*colD*, which was subjected to acetone (1 L \times 3) extraction and concentrated in vacuo. The residue (200 mL) was subjected to extraction in ethyl acetate (500 mL \times 3) to yield a brown oily extract. The combined organic layers (1.4 g) was analyzed by GC-MS and fractionated by silica gel with petroleum ether (PE) to afford G1–G15. Fractions G4 and G5 were combined (286 mg) and further purified using semipreparative HPLC. Intermediate compound **1** was obtained through separation on an ACE C18-PFP column (10 \times 250 mm), with a mobile phase consisting of 80% acetonitrile and 20% aqueous solution (t_R = 27.0 min, 11.0 mg).

FBMN-Guided Isolation and Identification of New Sesterterpenoids (2–5**).** FBMN has emerged as an advanced technique for the effective identification of target compounds from trace amounts of crude extracts.^{23,24} First, the AO-*orfA/colBCD* strain was cultivated on 1 g of rice medium for 5 days at 30 °C. The resulting culture was extracted with ethyl acetate (EtOAc), which was then concentrated in vacuo to yield 8.9 mg of dried extract. This extract was analyzed using a Shimadzu LC-20AD UPLC system connected to a Thermo Scientific Q Exactive Orbitrap mass spectrometer operating in positive electrospray ionization (ESI) mode. For the analysis, a 50 μ g/mL sample solution was prepared in MeOH. Chromatographic separation was performed on a Waters ACQUITY BEH C18 column (2.1 \times 100 mm, 1.7 μ m) with a water/ACN gradient. The data-dependent acquisition method involved a full MS survey scan (m/z 100–1200, 70,000 resolution), followed by higher-energy collisional dissociation (HCD) MS/MS scans (17,500 resolution, 40 eV collision energy) of the ten most abundant precursor ions.

Raw mass data were converted with MSConvert²⁹ and processed using MZmine 2,³⁰ filtering for ion peaks with $MS^1 > 3.0E6$ and $MS^2 > 3.0E3$ responsivity. The processed data for both the control (AO) and the engineered strain (AO-*orfA/colBCD*) were uploaded to the Global Natural Products Social (GNPS) platform for FBMN (Workflow version release_28.2) with a Minimum Pairs Cosine threshold of 0.75. From the network, 331 nodes in the m/z range of 300–500 were selected for further investigation. This range was targeted based on the predicted molecular weight of intermediate compound **1** after the potential addition of one to five oxygen atoms by post-tailoring enzymes. Raw data files are available at GNPS under the following task ID (<https://gnps.ucsd.edu/ProteoSAFe/status.jsp?task=76d8d88001c64bb7adee22ad5e2e2f7d>).

To isolate and identify the tailored products, the fermentation of AO-*orfA/colBCD* transformant was carried out in 50 kg rice medium (each containing 80 g rice, 120 mL water and 0.01% adenine), with stationary incubation at 30 °C for 27 days. The sample was exhaustively extracted with EtOAc and concentrated to yield a crude extract (25.7 g) was fractionated by normal phase silica gel chromatography using a gradient of DCM-MeOH (100% DCM, DCM:MeOH with ratios 99:1, 98:2, 97:3, 96:4, 95:5, 9:1, 7:3, 1:1, and 100% MeOH) as the mobile phase, resulting in ten subfractions (G1–G10). Based on characteristic UV absorption and LC-HRMS analysis, potential novel analogs of colcerepene were identified in G3 and G4. The two fractions were combined (5.7 g) and further separated using reversed-phased silica gel column with a MeOH–H₂O gradient (0%, 20%, 40%, 60%, 80%, 85%, 90%, 95%, and 100% MeOH) to give 9 subfractions RG1–RG9. After drying in vacuo, RG5 (92.7 mg) was subjected to semipreparative HPLC on an ACE C18 column (10 \times 250 mm), and eluted gradiently from 40% ACN–H₂O; 60% ACN–H₂O (20 min); and 99% ACN–H₂O (25 min). This process yielded **2** (3.5 mg, t_R = 26.9 min) and **3** (8.6 mg, t_R = 28.5 min). RG6 (114.2 mg) was purified by RP-HPLC on an ACE C18-PFP column (10 \times 250 mm) with a gradient elution (4.0 mL/min): 0 min, 55% ACN–H₂O; 20 min, 70% ACN–H₂O; and 25 min 99% ACN–H₂O. This yielded **4** (1.9 mg, t_R = 23.9 min) and **5** (1.7 mg, t_R = 25.5 min).

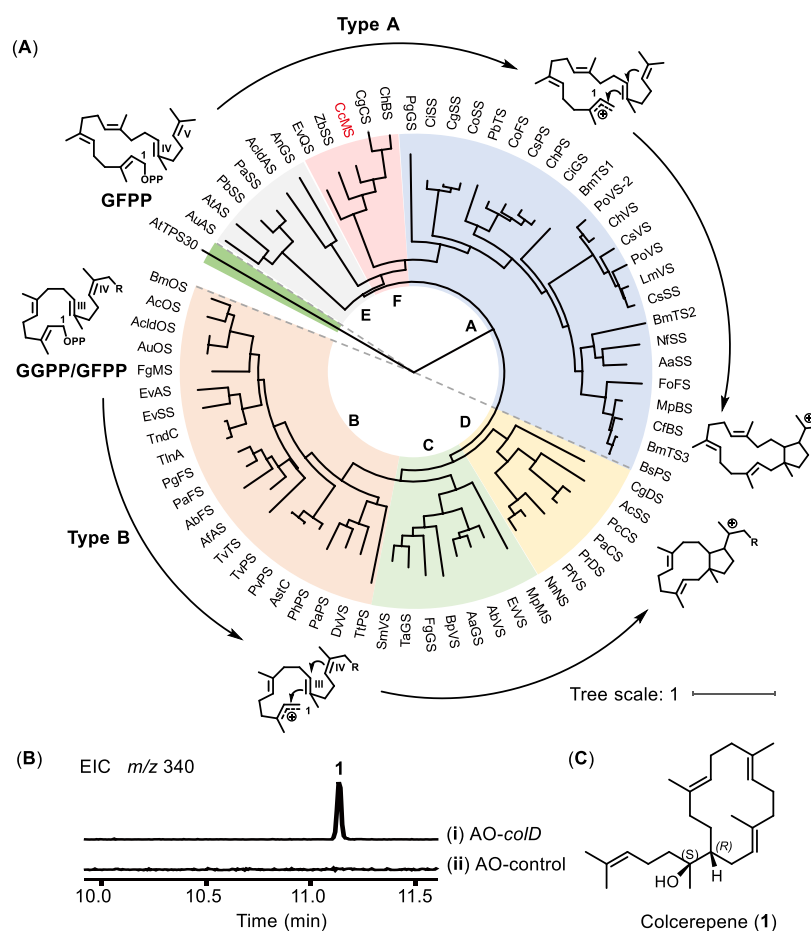


Figure 1. Bioinformatic analysis and heterologous expression of CcMS. (A) Maximum Likelihood phylogenetic tree of TC domains of 76 reported BFTPSs and the putative BFTPS CcMS from *C. cereale* 00173. BFTPSs in this study are indicated by red, and the reported ones are indicated by black. The bar represents 1 nucleotide substitutions per site. (B) GC-MS profiles of metabolites from AO-*colD* (i) and AO monitoring (ii). (C) Structures of colcerepenone, and key 2D NMR correlations of colcerepenone (1).

Colcerepenone (1): Colorless oil. $[\alpha]_D^{27} = -156.7$ (c 0.36, CHCl_3). ^1H NMR and ^{13}C NMR data, see Table S4; HR-ESI-MS m/z 340.3134 $[\text{M} - \text{H}_2\text{O}]^+$ (calcd. for $\text{C}_{25}\text{H}_{40}$, 340.3127) (Figure S2).

Colcerepenoid A (2): Colorless oil. $[\alpha]_D^{27} = -91.7$ (c 0.36, CHCl_3). ^1H NMR and ^{13}C NMR data, see Table S6; HR-ESI-MS m/z 373.3116 $[\text{M} - \text{H}_2\text{O} + \text{H}]^+$ (calcd. for $\text{C}_{25}\text{H}_{42}\text{O}_3$, 373.3107, Δ 3.876 ppm) (Figure S12).

Colcerepenoid B (3): Colorless oil, $[\alpha]_D^{27} = -84.1$ (c 0.64, CHCl_3). ^1H NMR and ^{13}C NMR data, see Table S7; HR-ESI-MS m/z 373.3114 $[\text{M} - \text{H}_2\text{O} + \text{H}]^+$ (calcd. for $\text{C}_{25}\text{H}_{42}\text{O}_3$, 373.3107, Δ 3.550 ppm) (Figure S20).

Colcerepenoid C (4): Colorless oil, $[\alpha]_D^{27} = -196.8$ (c 0.19, CHCl_3). ^1H NMR and ^{13}C NMR data, see Table S8; HR-ESI-MS m/z 357.3166 $[\text{M} - \text{H}_2\text{O} + \text{H}]^+$ (calcd. for $\text{C}_{25}\text{H}_{42}\text{O}_2$, 357.3157, Δ 3.995 ppm) (Figure S27).

Colcerepenoid D (5): Colorless oil, $[\alpha]_D^{27} = -102.7$ (c 0.22, CHCl_3). ^1H NMR and ^{13}C NMR data, see Table S9; HR-ESI-MS m/z 357.3167 $[\text{M} - \text{H}_2\text{O} + \text{H}]^+$ (calcd. for $\text{C}_{25}\text{H}_{42}\text{O}_2$, 357.3157, Δ 3.909 ppm) (Figure S35).

Rh₂(OCOCF₃)₄-Induced CD Spectra to Determine the Absolute Configuration of 1. Compound 1 (0.5 mg) was dissolved in 1 mL of chloroform and the original CD spectrum was immediately recorded. Subsequently, Rh₂(OCOCF₃)₄ (2 mg) was reacted with 1 in chloroform, and the CD spectra of the Rh-complexes were recorded until a stable state was achieved (approximately 20 min). The data collected for the Rh-complexes were corrected by subtracting the inherent CD spectrum. The absolute configuration of C-15 was determined by analyzing the sign of the E band around 350 nm in the induced CD spectrum.^{31,32}

Preparation of MTPA Esters to Determine the Absolute Configuration of 2, 3, and 5. MTPA esters were prepared by reacting compound 3 (1 mg) with 180 μL of deuterated pyridine for 0.5 h, followed by the addition of R-(-)-MTPA chloride (10 μL) to obtain 3a, and with S-(+)-MTPA chloride to obtain 3b. Similarly, compounds 2a/2b and 5a/5b were obtained from compounds 2 and 5 (0.5 mg each) using the same procedure.

Chemical Computation Details. All theoretical calculations were performed using density functional theory (DFT).³³ A preliminary conformational search was conducted with Sybyl-X 2.0 software. The resulting ground-state geometries were subsequently optimized at the B3LYP/6-31G(d) level. Finally, magnetic shielding constants for the stable conformers were calculated at the B3LYP/6-311+G(2d, p) level.

Precursor Feeding Experiment. The biotransformation assay using compound 4 and 5 as the substrate was conducted following the procedure described previously.³⁴ The AO, AO-*colB*, and AO-*colC* transformants were cultivated for 2 days at 30 °C. Biotransformation assays were then conducted using compound 4 and 5 as substrates. For compound 4, 1 mL of PBS buffer containing 300 μg of substrate (DMSO solution) was applied to the surface of both blank MPY and AO-*colB*. Similarly, for compound 5, 1 mL of PBS buffer containing 300 μg of substrate (DMSO solution) was applied to the surface of blank MPY and AO-*colC*. Following incubation at 30 °C for 2 days, the samples were extracted with EtOAc. The resulting organic layer was dried, reconstituted in MeOH, and then profiled using LC-HRMS.

Antimicrobial Assays. Antimicrobial assays were conducted following the antimicrobial susceptibility testing standards outlined

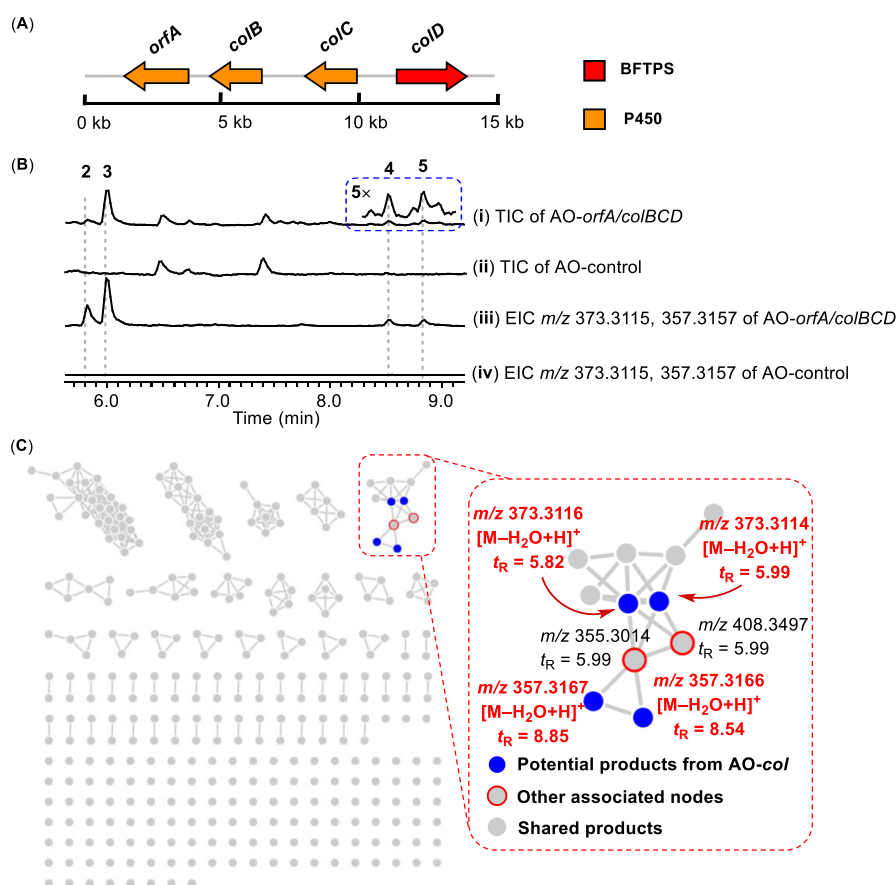


Figure 2. Heterologous expression of the *col* gene cluster. (A) Gene organization of the proposed colcerepenoids biosynthetic cluster. (B) LC-HRMS profiles of metabolites from TIC of AO-*orfA/colBCD* (i); AO-control (ii) EIC 373.3115 and 357.3157 of AO-*orfA/colBCD* (iii) and EIC 373.3115 and 357.3157 of AO-control (iv). (C) Overview of the molecular networking generated from LC-HRMS data sets of the AO-*col* gene cluster.

by the Clinical and Laboratory Standards Institute (CLSI) and in accordance with previous report.³⁵ The methicillin-resistant *S. aureus* strain (MRSA) (clinical strain from Chaoyang Hospital, Beijing, China),³⁶ *E. coli* ATCC11775, *Paratyphoid fever*, *Bacillus cereus*, *Salmonella enteritidis* C50336, and *Mycobacterium smegmatis* MC2155 was employed for testing.

Antineuroinflammatory Activity In Vitro. The in vitro anti-inflammatory assay followed the methods of Yang et al.³⁷ Nitric oxide production was quantified through nitrite accumulation analysis using a commercial Griess assay system (Thermo Fisher, Shanghai). Spectrophotometric measurements were conducted at 560 nm using a microplate reader.

Cell Cytotoxicity Assay. Cell viability was assessed using a Cell Counting Kit-8 (CCK-8; AC Biotechnology Co., Ltd., Qingdao, China) according to the manufacturer's protocol.³⁸ Absorbance was measured at 450 nm using a microplate reader (MULTISKAN MK3), with a reference wavelength of 650 nm to correct for nonspecific absorption. Cell viability (%) was calculated as

$$\text{viability} = (A_{\text{sample}} - A_{\text{blank}}) / (A_{\text{vehicle control}} - A_{\text{blank}}) \times 100$$

Where A_{sample} , $A_{\text{vehicle control}}$, and A_{blank} represent the absorbance of treated cells, vehicle-only control cells (100% viability), and medium + CCK-8 reagent without cells, respectively.

Statistical Assay. Data were derived from independent experiments performed in triplicate replicates and expressed as mean \pm SD. Statistical significance was determined by one-way ANOVA with Tukey's posthoc test using GraphPad Prism 8.0 software (GraphPad, La Jolla, CA, USA) (* $p < 0.05$).

RESULTS AND DISCUSSION

Bioinformatic Analysis and Discovery of a New Macrocyclic Sesterterpene Synthase. Macrocyclic sesterterpenoids exhibit unique pharmacological effects due to their rigid frameworks and specific interactions with biological targets, often demonstrating combined antimicrobial, anti-inflammatory, and anticancer activities.¹² While fungi are major sources of natural terpenoids, most known macrocyclic diterpene synthases are plant-derived,^{11,39,40} with few reported in fungi. To date, only one bifunctional terpene synthase, CgCS from *C. gloeosporioides*, has been characterized to catalyze the formation of a macrocyclic triterpene scaffold.²⁰

To explore novel biosynthetic analogs, we employed CgCS as a probe for a BLASTp alignment against the amino acid sequence of the congeneric fungus *C. cereale* 00173. This search identified a BFTPS sharing 69.5% identity (52.2% similarity) with CgCS. This enzyme, predicted to encode 767 amino acids, retains the conserved terpene synthase motifs: the N-terminal ⁹⁵DDXXD/E⁹⁹ motif and ²²⁸NSE/DTE²³⁶ triad in the TC domain, along with C-terminal ⁴⁹⁴DDXXD⁴⁹⁸ and ⁶²³DDXXD⁶²⁷ motifs in the PT domain (Figure S1). Based on the phylogenetic framework previously established by Hideaki Oikawa,⁴¹ phylogenetic analysis revealed that this BFTPS found in *C. cereale* 00173 belongs to clade F of type A synthases, a rare group with only four reported members (Figure 1A).

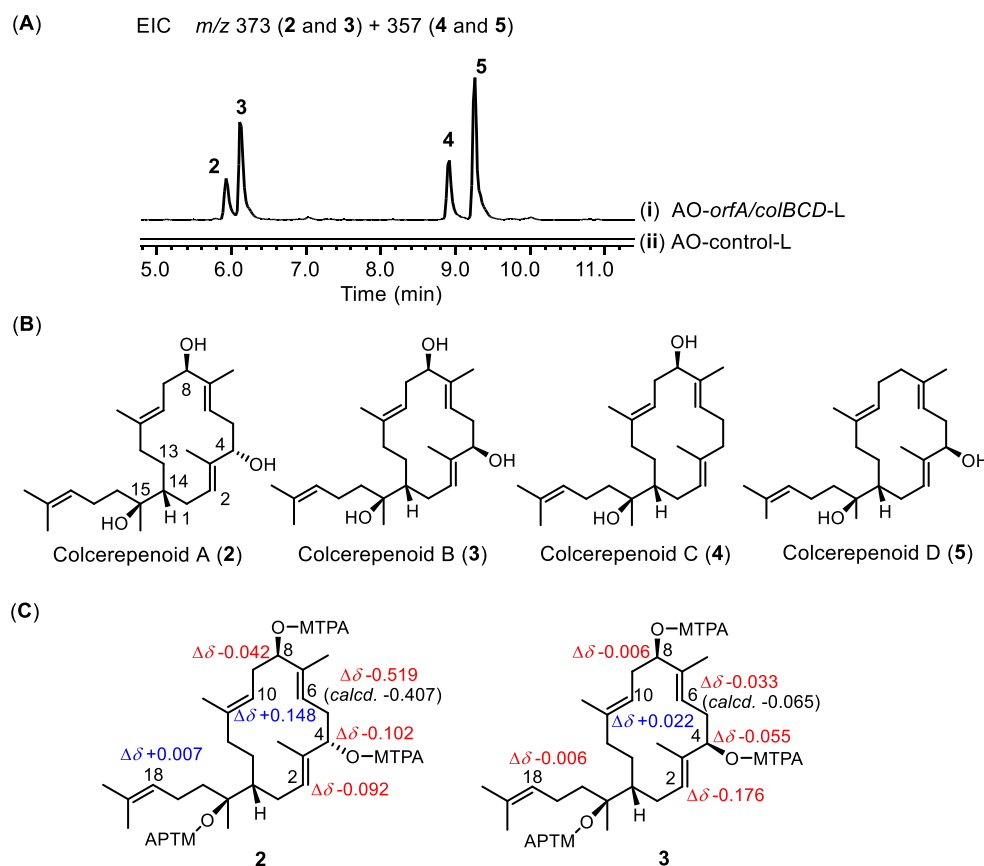


Figure 3. Large-scale fermentation of AO-*orfA*/colBCD and the structures of colcerepenoids. (A) LC-HRMS profiles of metabolites from large-scale fermentation (marked as L) extracts of AO-*orfA*/colBCD (i) and AO-control (ii). Chromatograms were extracted at m/z 357 and 373 [$M - H_2O + H$] $^+$. (B) Structures of colcerepenoids A–D (2–5). (C) $\Delta\delta$ -Values ($\delta_S - \delta_R$) of (S)- and (R)-MTPA esters 2 and 3.

To uncover the function of this BFTPS, the corresponding gene (*colD*) was expressed in *A. oryzae*. GC–MS analysis of extracts from the recombinant strain (AO-*colD*) revealed a unique product with a molecular ion at m/z 340, which was absent in the control strain (AO) (Figure 1B). Subsequent purification by silica gel chromatography and HPLC yielded the major product, compound 1, as a colorless oil with $[\alpha]_D^{27} -156.7$ (c 0.36, $CHCl_3$). HR-EI-MS established its molecular formula as $C_{25}H_{42}O$, indicating five degrees of unsaturation (found 340.3134 [$M - H_2O$] $^+$, calcd. for 340.3127) (Figure S2). The 1H NMR, ^{13}C NMR, and HSQC spectra of 1 revealed 25 carbon signals, which included six methyl groups ($\delta_{C/H}$ 15.9/1.65, 15.7/1.58, 16.2/1.65, 25.1/1.39, 18.1/1.65, and 26.2/1.70), nine methylene groups, one methine, four trisubstituted double bonds (δ_C 132.9/128.1, 133.2/126.7, 134.7/125.5, and 131.2/126.4), and one sp^3 quaternary carbon (δ_C 74.7). The chemical shift of 74.7 ppm for the quaternary carbon indicates the presence of an additional hydroxyl group in the structure. Based on its five unsaturation degrees, the four double bonds suggest that compound 1 could be a monocyclic sesterterpene. The 1D NMR signals of 1 closely resembled those of (14*S*,15*R*,2*E*)-15-hydroxy- α -cericerene, with both compounds featuring a side chain shortened by one isoprene unit relative to colleterpenol.^{20,42} The 1H – 1H COSY and HMBC correlations further establish the 14-membered macrocyclic structure (Table S4 and Figures S3–S7). The relative configuration of 1 was partially elucidated through the analysis of key NOESY signals. All double bonds were assigned as *E*-configuration based on the correlations of H-2/H-4, H-

1b/H-20, H-6/H-8, H-5/H-21, H-10/H-12a, and H-9/H-22 (Figure S8). Thus, the planar structure of 1 was fully established as a 14-membered macrocyclic sesterterpene and was found to be identical to that of known sesterterpene (14*S*,15*R*,2*E*)-15-hydroxy- α -cericerene (Figure S9).⁴²

However, the specific rotation of 1 was opposite to that of the known compound (+106.7), suggesting it was an enantiomer.¹² The absolute configuration at C-15 was definitively established through additional circular dichroism measurements induced by $Rh_2(OCOFCF_3)_4$. The positive Cotton effect observed at 350 nm for the Rh-complex further supported a 1*S*S** configuration based on the ‘b*S*’ bulkiness (Figure S10).^{31,32} The further calculated ECD spectrum for the (14*R*,15*S*)-1 isomer shows excellent agreement with the experimental spectrum, while the spectrum for the (14*S*,15*S*) epimer showed an inverted or poorly matching curve. (Figure S11). Thus, the absolute structure of compound 1 was unambiguously determined to be 14*R*,15*S*. This macrocyclic sesterterpene was named colcerepene (Figure 1C), and then the BFTPS responsible for its biosynthesis was designated CcMS (*Colletotrichum cereale* Macrocylic Sesterterpenoid Synthase).

FBMN-Guided Discovery of New Sesterterpenoids Colcerepenoids A–D (2–5). To expand the chemical diversity of post-tailored products of 1, we analyzed the gene cluster associated with CcMS. Bioinformatics analysis revealed three adjacent cytochrome P450 monooxygenase genes (*orfA*, *colB*, and *colC*), suggesting that their coexpression with CcMS could yield oxidized derivatives of colcerepene (1). OrfA is

homologous to ARMGADRAFT_1018417, which catalyzes hydroxylation in the melleolide biosynthesis.^{43,44} ColB is similar to EqxH, part of the equisetin biosynthetic gene cluster.⁴⁵ ColC shows high similarity to Hmp1, a post-modification enzyme of hypothemycin (Figure 2A and Table S1).⁴⁶ All these genes are present in characterized fungal secondary metabolic pathways. To explore these potential postmodification products, a transformant harboring all four genes (AO-*orfA*/colBCD) was constructed. We run FBMN for the rapid and targeted detection of trace colcerepenes related sesterterpenoids from microscale cultures of the transformant.^{23,24}

Microculture extracts (1 g rice medium) were analyzed by LC-HRMS and data were subjected to FBMN analysis. Based on the hypothesis that the P450 enzymes would introduce oxygen atoms to colcerepenes (**1**), the LC-HRMS analysis was focused on a mass range of m/z 340–518, resulting in 331 remaining nodes in the network. The FBMN analysis of the AO-*orfA*/colBCD extract successfully identified four nodes of interest absent in the control strain. These included 2 nodes at m/z 373.3115 $[M - H_2O + H]^+$ (calcd. for $C_{25}H_{41}O_3$, $t_R = 5.82$ min and $t_R = 5.99$ min) and 2 nodes with m/z 357.3157 $[M - H_2O + H]^+$ (calcd. for $C_{25}H_{42}O_2$, $t_R = 8.54$ min and $t_R = 8.85$ min), corresponding to di- and monohydroxylated derivatives of colcerepenes (**1**), respectively (Figure 2B,C). Guided by the FBMN analysis, large-scale fermentation (50 kg rice medium) of AO-*orfA*/colBCD strain was performed, leading to the isolation and characterization of four new 14-membered macrocyclic sesterterpenoids (**2**–**5**) (Figure 3A). NMR analysis confirmed that all four compounds retained the 14-membered macrocyclic ring system of colcerepenes (**1**) (Figure 3B).

Compounds **2** and **3** were identified as isomers, with NMR data indicating that both were dihydroxylated derivatives of **1**, with hydroxyl groups located at C-4 and C-8. The 1D NMR signals of **2** closely resembled those of compound **1**, with two additional signals corresponding to hydroxyl groups ($\delta_{C/H}$ 78.1/4.50, 77.8/4.35). Hydroxylation at C-4 and C-8 was confirmed by 1H – 1H COSY correlations of H-4/H-5 and H-8/H-9, as well as HMBC correlations of H₃-20/C-4, H-2/C-4, and H₃-21/C-8 (Table S6 and Figures S13–S18). The 1H and ^{13}C NMR data of compound **3** shared an identical planar structure with compound **2**, featuring hydroxyl groups at C-4 and C-8 (Table S7 and Figures S21–S25). Based on the analysis of key NOESY signals, all double bonds of **2** were assigned as *E*-configuration, as confirmed by the correlations of H-2/H-4, H-1b/H-20, H-6/H-8, H-5/H-21, H-10/H-12a, and H-9a/H-22 (Figure S19). Compound **3** exhibits a double bond geometry consistent with that of **2** (Figure S26).

To determine their absolute configurations, TD-DFT-based ECD and ^{13}C NMR calculations for the two C-4 epimers were performed. However, the calculated CD spectra for both epimers were dominated by the core scaffold and exhibited nearly identical trends (Figure S54), making them unsuitable for differentiation, and the ^{13}C NMR calculations of **2** and **3** afforded identical DP4 probability (Tables S11 and S12). Subsequently, the MTPA esters of **2** and **3** (**2a**, **2b**, **3b** and **3d**, respectively) were prepared by reacting with *R*-(–)-MTPA chloride and *S*-(+)-MTPA chloride, respectively.⁴⁷ Based on the $\Delta\delta$ ($\delta_S - \delta_R$) at H-6 and H-10, the absolute configuration at C-8 of **2** and **3** were both determined as *R* configuration and *S* configuration at C-2. Although the chirality at C-4 could not be directly determined from this analysis, the opposing trends

in the $\Delta\delta$ values surrounding C-4 in **2** and **3** suggested they were C-4 epimers (Figure 3B, S19, S26, and S42–S47). This was further validated by DFT-based quantum chemical calculations of the 1H NMR chemical shifts, which exhibited a consistent $\Delta\delta$ trend at the H-6 position, in agreement with the experimental observations (Figures 3C, S55, and S56, Table S10). Based on these combined analyses, the absolute configuration of **2** was assigned as 4*S*,8*R*,14*R*,15*S*, and the absolute configuration of **3** was assigned as 4*R*,8*R*,14*R*,15*S*.

Compound **4** was a monohydroxylation product of **1**, with the additional hydroxyl group ($\delta_{C/H}$ 78.2/4.38) (Table S8) positioned at C-8, as confirmed by 1H – 1H COSY correlations of H-8/H-9 and HMBC correlations of H₃-21/C-8 (Figure 3B and Figures S28–S33). Since subsequent feeding experiments identified Compound **4** as the biosynthetic precursor to **2** and **3**, its absolute configuration at C-8 was determined as *R*, and double bond geometry was consistent with that of **2** and **3** (Figure 5C and S34).

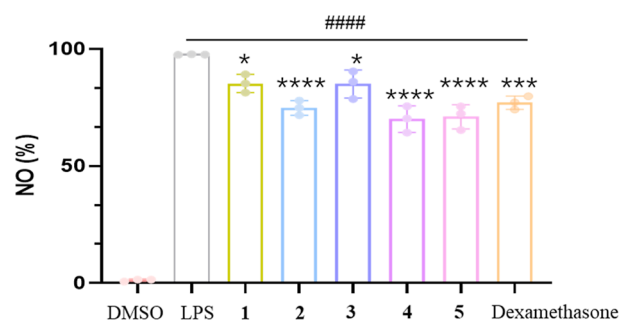


Figure 4. Inhibitory effects of compounds **1**–**5** against LPS-induced NO production in BV2 cells. Mean \pm SD of four replicates is shown. * $p < 0.05$, *** $p < 0.001$, **** $p < 0.0001$ with the LPS group. ##### $p < 0.0001$ with the control group.

The presence of a hydroxyl group at C-4 in compound **5** was confirmed through HMBC correlations of H₃-20/C-4 and H-2/C-4 (Figures S36–S40). All double bonds of **5** were assigned as *E*-configuration based on the key NOESY correlations of H-2/H-4, H-1a/H-20, H-6/H-8, H-5/H-21, H-10/H-12, and H-9/H-22 (Figure S41). Subsequent Mosher ester analysis⁴⁷ was used to determine the absolute configuration of C-4 as *R* (Figures 3B and S48–S51), establishing the absolute configuration of **5** as 4*R*,14*R*,15*S*.

Biological Activity Evaluation of Colcerepenoids. The potential activities of the isolated compounds (**1**–**5**) was evaluated through a series of bioassays to determine their antimicrobial, antineuroinflammatory, and cytotoxic activities.

The antibacterial activities of compounds **1**–**5** were evaluated against a panel of common foodborne human pathogens. MRSA represents a severe public health threat due to its multidrug resistance, severely limiting treatment options and transforming routine infections into life-threatening conditions. Furthermore, its presence in livestock and the food chain presents a significant zoonotic risk, enabling difficult-to-treat foodborne outbreaks. This persistent pathogen underscores the urgent need for innovative antimicrobial solutions to mitigate its escalating burden on both agriculture and public health.⁴⁸ Antibacterial assays demonstrated that compound **1** exhibited significant inhibitory activity against a clinical MRSA strain with a minimum inhibitory concentration (MIC) of 6.25 μ M. In contrast, its hydroxylated derivatives showed reduced efficacy. Compounds **4** and **5** had MIC values

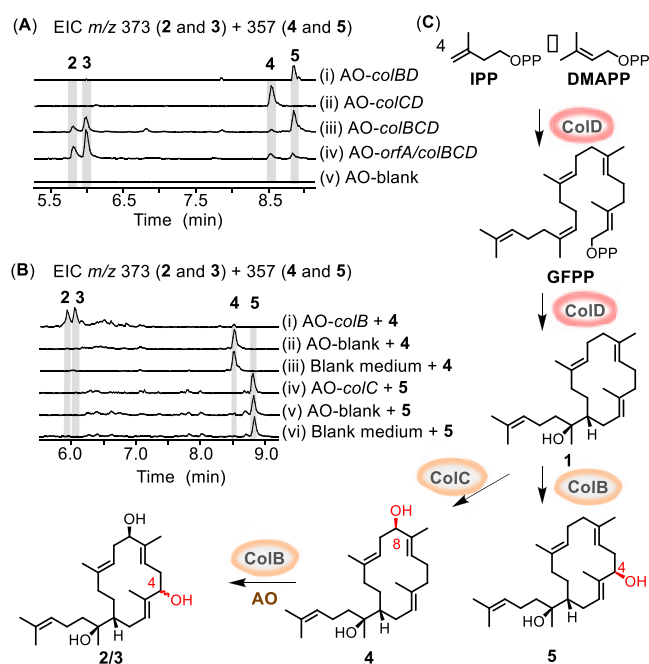


Figure 5. Gene function validation of *orfA*, *colB*, and *colC* in *A. oryzae*. (A) LC-HRMS profiles of extracts from AO-*colBD* (i), AO-*colCD* (ii), AO-*colBCD* (iii), AO-*orfA/colBCD* (iv), and AO-blank (v), chromatograms were extracted at m/z 373 + 357 [$M - H_2O + H$] $^+$. (B) LC-HRMS profiles of 4 fed to AO-*colB* (i), AO (ii), and blank medium (iii); LC-HRMS profiles of 5 fed to AO-*colC* (iv), AO (v), and blank medium (vi), chromatograms were extracted at m/z 373 + 357 [$M - H_2O + H$] $^+$. (C) Biosynthetic pathway of colcerepenoids in *A. oryzae*.

of 25 μ M, a 4-fold decrease in potency compared to compound 1.

In addition to MRSA, activity was assessed against *M. smegmatis* (a nonpathogenic surrogate for *M. tuberculosis*), which serves as a common surrogate for *M. tuberculosis*, the causative agent of tuberculosis.⁴⁹ Tuberculosis remains a significant global health threat, necessitating the discovery of novel therapeutic agents. Furthermore, *M. smegmatis* itself poses risks to food safety and agricultural systems. Its extreme tolerance to common disinfectants and its environmental persistence enables the contamination of water sources, soil, and food processing facilities. This resilience can lead to the cross-contamination of agricultural products, particularly dairy and produce, and contributes to the environmental spread of antimicrobial resistance (AMR) genes within food chains.^{50,51} In this work, compound 2 displayed moderate antibacterial activity against *M. smegmatis*, with an MIC of 12.5 μ M, while the positive control rifampicin had an MIC of 1.56 μ M (Table 1). However, none of the compounds exhibited any activity against *E. coli*, *S. paratyphoid*, *B. cereus*, and *S. enteritidis* (Table S13).

These results strongly suggests that the overall hydrophobicity of the colcerepene scaffold is a key determinant for its antibacterial potency. To quantitatively support this hypothesis, we have also calculated the logP values for these compounds using Chem3D (Table S14). It is plausible that, similar to many membrane-targeting agents, the efficacy of compound 1 (logP = 5.8) is associated with its ability to effectively insert into the lipid bilayer and perturb the cell membrane.^{52,53} Consequently, chemical modifications that increase hydrophilicity, such as the hydroxylations observed

Table 1. Antibacterial and Cytotoxicity Activities of 1–5

Compound	MIC (μ M)		Cell inhibition \pm SD (%) ^a at 20 μ M	
	MRSA	<i>m. smegmatis</i>	MKN-45	HepG2
1	6.25	>50	40.11 \pm 0.99%	46.31 \pm 1.67%
2	>50	12.5–25	25.73 \pm 0.38%	34.75 \pm 2.32%
3	>50	25–50	4.40 \pm 1.99%	19.40 \pm 0.41%
4	25	>50	15.12 \pm 2.99%	32.46 \pm 1.67%
5	25	>50	12.87 \pm 2.00%	38.99 \pm 1.96%
Van ^b	1.56	NT	NT	NT
Rfp ^b	NT	1.56	NT	NT
Dox ^b	NT	NT	88.72 \pm 0.73%	91.77 \pm 0.99%

^aCell inhibition rates are the mean \pm SD of three independent experiments at corresponding concentration. NT, not tested. ^bPositive control.

in 2–5 (logP range = 3.8–4.3), appear to impair this mechanism by altering the compound's optimal hydrophobic–hydrophilic balance and promoting membrane perturbation, leading to reduced antimicrobial activity (Table S14). Similar trends have been observed in other terpenoids, where postmodification processes modulate their biological functions. For instance, hydroxylated asperterpenoids have demonstrated increased hydrophilicity but diminished antibacterial activity, likely due to reduced interactions with bacterial proteins.⁵⁴

In addition to their antimicrobial activity, metabolites of fungi are increasingly recognized as a promising source of neuroprotective agents,⁵⁵ particularly newly discovered anti-inflammatory terpenoids.^{56,57} The enantiomer of compound 1 exhibits inhibitory effects on the inflammatory cytokines TNF- α and IL-6,⁴² which are involved in the induction of nitric oxide (NO) production. Therefore, we preliminarily assess the anti-inflammatory potential of compound 1 and its derivatives based on their inhibitory effects on NO production. The antineuroinflammatory potential of these compounds was assessed by evaluating their effects on LPS-induced nitric oxide (NO) production in BV2 microglial cells. Compounds 2, 4, and 5 demonstrated preliminary anti-inflammatory activity at 20 μ M, with NO inhibition rates of 25.1%, 29.6%, and 30.1%, respectively, and the remaining compounds showed relatively weak anti-inflammatory effects (Figure 4). However, these findings are preliminary and face two key limitations. First, the limited yield of colcerepenoids restricted testing to a single concentration (20 μ M), preventing IC₅₀ determination. Second, while these findings indicate moderate activity, the underlying mechanism of action remains unknown. A full mechanistic investigation, such as determining effects on pathways like NF- κ B signaling, iNOS/COX-2 expression, or cytokine release, was considered beyond the scope of this initial discovery-focused study. In follow-up studies, obtaining sufficient quantities of these compounds will be essential to both accurately determine their IC₅₀ values and elucidate their precise anti-inflammatory mechanisms.

Furthermore, the cytotoxicity of compounds 1–5 was evaluated against human stomach (MKN-45) and liver (HepG2) cancer cell lines, using doxorubicin hydrochloride as the positive control. Only Compound 1 exhibited weak inhibition against the growth of MKN-45 and HepG2 cells by 40.11 \pm 0.99% and 46.31 \pm 1.67%, respectively, at 20 μ M (Table 1). The hydroxylated derivatives 2–5 showed markedly lower cytotoxicity (Table S16). In our study, an integrated structure–activity relationship (SAR) analysis revealed a

divergent trend. The parent compound, colcerepene (1), showed the most potent antibacterial activity but was inactive in anticancer assays. In contrast, its hydroxylated derivatives (2–5) exhibited reduced antibacterial potency but gained weak anticancer activities, particularly against HepG2 and MKN-45 cell lines. This suggests that structural modifications, such as hydroxylation, critically alter the compound's hydrophobic–hydrophilic balance. This provides a clear strategy for optimization: it may be possible to enhance bacterial specificity and therapeutic index by maintaining hydrophobicity (to keep antibacterial activity) while concurrently ensuring low cytotoxicity to host cells. These findings emphasize the significance for a more systematic SAR analysis, potentially through the design and synthesis of targeted analogs in future studies.

Biosynthetic Pathway Elucidation of the Colcerepenoids. To elucidate the biosynthetic pathway of colcerepenoids 2–5, a series of engineered *A. oryzae* strains were constructed and the ethyl acetate extracts from these transformants were analyzed by LC-HRMS. Coexpression of *colB* and *colD* (strain AO-*colBD*) and *colC* and *colD* (strain AO-*colCD*) revealed that P450s ColB and ColC hydroxylated compound 1 at C-4 and C-8, resulting in compounds 5 and 4, respectively (Figure 5A, traces i and ii). The coexpression of all three P450s with *colD* (strain AO-*colBCD*) produced all four hydroxylated derivatives (2–5), confirming that *orfA* is not involved in their biosynthesis (Figure 5A, traces iii and iv). No additional products were detected in the AO-blank crude extracts, indicating that the AO endogenous enzyme did not contribute to the formation of compounds 2–5 (Figure 5A, trace v).

To identify the precursors of the dihydroxylated products 2 and 3, substrate feeding experiments were performed. When compound 4 was fed to the AO-*colB* strain, both 2 and 3 were detected, indicating that ColB catalyzes hydroxylation at C-4 to produce these C-4 epimers from 4. In contrast, feeding compound 5 to the AO-*colC* strain did not yield any further products (Figure 5B). These findings establish that colcerepenoid C (4) is the key intermediate in the pathway leading to both colcerepenoid A (2) and B (3). However, P450 enzymes typically exhibit high stereospecificity, with an asymmetric active site structure that allows substrates to bind in a specific conformation, yielding a single stereoisomer. Our literature review revealed a potential parallel: the P450 product 5-*epi*-armilol is converted to the unstable tsugicolone B by a short-chain dehydrogenase/reductase (SDR), which is then reduced to its epimer, armilol, by another SDR.⁵⁸ This suggests that compound 2 is not a direct product of ColB, but is instead derived from the initial P450 product (compound 3) through a similar epimerization process involving endogenous AO host enzymes. This mechanism would explain the resulting pair of C-4 epimers. A proposed biosynthetic pathway for the colcerepenoids is illustrated in Figure 5C: The PT domain of CcMS catalyzes the head-to-tail condensation of isopentenyl pyrophosphate (IPP) and dimethylallyl pyrophosphate (DMAPP) to produce the C₂₅ linear precursor geranylarnesyl pyrophosphate (GFPP), which is subsequently cyclized by the TC domain to yield 1. The compound 1 are then hydroxylated by the P450 ColB and ColC to generate 5 and 4, respectively. Compound 4 is further transformed by ColB and endogenous AO host enzymes, affording a pair of C-4 epimers.

However, we acknowledge that the precise functions of the P450 tailoring enzymes in this study were inferred from in vivo

heterologous expression and feeding experiments. Further validation via in vitro enzymatic assays would be ideal, but this is currently impeded by the significant technical challenges of purifying these membrane-associated fungal enzymes.

Terpenoids, known for their medicinal properties, have demonstrated a wide range of unique biological activities, such as artemisinin and paclitaxel.^{59,60} Among terpenoids, macrocyclic structures, have gained significant interest due to their diverse bioactive properties, including antimicrobial, anti-inflammatory, and anticancer activities. These compounds, which are primarily found in plants and fungi, have shown promise in a range of therapeutic applications, such as durumolides, derived from *Lobophytum durum* Tixier-Durivault, demonstrate potent activity against *Salmonella enterica* subsp. *enterica* serovar Typhimurium, with inhibition rates exceeding those of the positive control, ampicillin.⁶¹ Similarly, lobophytone T, isolated from the Chinese soft coral *L. pauciflorum* Ehrenberg, exhibits antimicrobial properties, effectively inhibiting the growth of *S. aureus*, *Streptococcus pneumoniae*, and yeast.⁶² However, regarding the colcerepenoids identified in this study, a direct comparison to nonmacrocyclic analogs, which would definitively determine the role of the 14-membered ring in conferring activity, is not yet available. These analogs were not isolated from our strain and their synthesis is nontrivial. Therefore, while we have identified preliminary activity for this scaffold, the specific contribution of the macrocyclic ring itself (versus a linear precursor) remains unknown and presents a key objective for future investigations.

In conclusion, this study successfully employed a strategy combining genome mining and heterologous expression to uncover the biosynthetic pathway of a new family of macrocyclic sesterterpenoids in *C. cereale* 00173. A novel bifunctional terpene synthase, CcMS, was identified as the catalyst that synthesizes the core scaffold, colcerepene (1), which was further decorated by downstream P450 enzymes to yield four new hydroxylated derivatives (2–5). Biological evaluation demonstrated that colcerepene (1) exhibits potent inhibitory activity against the drug-resistant pathogen MRSA, while its hydroxylated derivatives (2, 4, and 5) display moderate antineuroinflammatory effects. The elucidation of this pathway provides a molecular foundation for the target engineering of these compounds through synthetic biology. This work not only expands the chemical diversity of macrocyclic sesterterpenoids but also highlights their dual potential as leads for developing agents against foodborne pathogens and as functional ingredients that can enhance health through neuroinflammatory regulation.

■ ASSOCIATED CONTENT

Supporting Information

The Supporting Information is available free of charge at <https://pubs.acs.org/doi/10.1021/acs.jafc.5c11512>.

The molecular network grouping MS/MS data, HR-EI-MS spectrum of 1, HR-ESI-MS spectra of 2–5; 1D and 2D NMR spectra of 1–5; ECD calculation details, and antimicrobial activities of compounds against human pathogenic microbes (PDF)

■ AUTHOR INFORMATION

Corresponding Authors

Lan Jiang – Department of Cardiothoracic Surgery, Children's Hospital of Nanjing Medical University, Nanjing 210093, China; Neuroregeneration and Stem Cell Programs, Institute for Cell Engineering, Johns Hopkins University School of Medicine, Baltimore, Maryland 21205, United States; Email: zhuguoliang@ecust.edu.cn

Guoliang Zhu – State Key Laboratory of Bioreactor Engineering, East China University of Science of Technology, Shanghai 200237, China; orcid.org/0000-0002-6628-8874; Email: jianglan0426@163.com

Authors

Keying Lan – State Key Laboratory of Bioreactor Engineering, East China University of Science of Technology, Shanghai 200237, China

Zhennan Wang – State Key Laboratory of Bioreactor Engineering, East China University of Science of Technology, Shanghai 200237, China

Kangjie Lv – State Key Laboratory of Bioreactor Engineering, East China University of Science of Technology, Shanghai 200237, China

Cuiping Xing – State Key Laboratory of Bioreactor Engineering, East China University of Science of Technology, Shanghai 200237, China

Xiaoying Li – State Key Laboratory of Bioreactor Engineering, East China University of Science of Technology, Shanghai 200237, China

Qiang Yin – State Key Laboratory of Bioreactor Engineering, East China University of Science of Technology, Shanghai 200237, China

Yuwei Chen – College of Biotechnology and Pharmaceutical Engineering, Nanjing Tech University, Nanjing 211816, China

Xuming Mo – Department of Cardiothoracic Surgery, Children's Hospital of Nanjing Medical University, Nanjing 210093, China; State Key Laboratory of Reproductive Medicine and Offspring Health, Nanjing Medical University, Nanjing 210093, China

Xiaobo Mao – Neuroregeneration and Stem Cell Programs, Institute for Cell Engineering, Johns Hopkins University School of Medicine, Baltimore, Maryland 21205, United States; orcid.org/0000-0001-6587-556X

Weijie Wu – Jiangsu Alipay Bio-technology Co., Ltd, Nantong 226009, China

Tom Hsiang – School of Environmental Sciences, University of Guelph, Guelph, Ontario N1G2W1, Canada

Lixin Zhang – State Key Laboratory of Bioreactor Engineering, East China University of Science of Technology, Shanghai 200237, China

Huanqin Dai – Chinese Academy of Sciences Key Laboratory of Pathogenic Microbiology and Immunology, Institute of Microbiology, Chinese Academy of Sciences, Beijing 100101, China

Xueting Liu – State Key Laboratory of Bioreactor Engineering, East China University of Science of Technology, Shanghai 200237, China; orcid.org/0000-0002-1322-8253

Complete contact information is available at:
<https://pubs.acs.org/10.1021/acs.jafc.5c11512>

Funding

We gratefully acknowledge financial support from Jiangsu Health International Exchange Program, Shanghai Sci-Tech Inno Center for Infection & Immunity (SSIII-2024A01 and SSIII-2024A02), Shanghai Municipal Science and Technology Major Project, the National Key Research and Development Program of China (2020YFA0907800 and 2019YFA0906200), the National Natural Science Foundation of China (21977029, 81903529), the Open Project Funding of the State Key Laboratory of Bioreactor Engineering, and the 111 Project (B18022).

Notes

The authors declare no competing financial interest.

■ ACKNOWLEDGMENTS

We sincerely thank Prof. Hideaki Oikawa at Hokkaido University for his kind support of our project. And the support of Natural Science and Engineering Research Council of Canada to Prof. T. Hsiang, which funded the genome sequencing and assembly of *C. cereale* 00173.

■ REFERENCES

- (1) Boucher, H. W.; Talbot, G. H.; Bradley, J. S.; Edwards, J. E.; Gilbert, D.; Rice, L. B.; Scheld, M.; Spellberg, B.; Bartlett, J. Bad Bugs, No Drugs: No ESKAPE! An Update from the Infectious Diseases Society of America. *Clin. Infect. Dis.* **2009**, 48 (1), 1–12.
- (2) Shoaib, M.; Aqib, A. I.; Muzammil, I.; Majeed, N.; Bhutta, Z. A.; Kulyar, M.; Fatima, M.; Zaheer, C.; Muneer, A.; Murtaza, M.; Kashif, M.; Shafqat, F.; Pu, W. MRSA compendium of epidemiology, transmission, pathophysiology, treatment, and prevention within one health framework. *Front. Microbiol.* **2023**, 13, 1067284.
- (3) Turner, N. A.; Sharma-Kuinkel, B. K.; Maskarinec, S. A.; Eichenberger, E. M.; Shah, P. P.; Carugati, M.; Holland, T. L.; Fowler, V. G. Methicillin-resistant *Staphylococcus aureus*: an overview of basic and clinical research. *Nat. Rev. Microbiol.* **2019**, 17 (4), 203–218.
- (4) Aung, K. T.; Hsu, L. Y.; Koh, T. H.; Hapuarachchi, H. C.; Chau, M. L.; Gutiérrez, R. A.; Ng, L. C. Prevalence of methicillin-resistant *Staphylococcus aureus* (MRSA) in retail food in Singapore. *Antimicrob. Resist. Infect. Control* **2017**, 6 (1), 94.
- (5) González-Machado, C.; Alonso-Calleja, C.; Capita, R. Methicillin-Resistant *Staphylococcus aureus* (MRSA) in Different Food Groups and Drinking Water. *Foods* **2024**, 13 (17), 2686.
- (6) Xing, L.; Cheng, M.; Wang, S.; Jiang, J.; Li, T.; Zhang, X.; Yang, J.; Tian, Y.; Liu, W. Methicillin-resistant *Staphylococcus aureus* contamination in meat and meat products: a systematic review and meta-analysis. *Front. Microbiol.* **2025**, 16, 1636622.
- (7) Kwasuji, H.; Nagaoka, K.; Tsuji, Y.; Kimoto, K.; Takegoshi, Y.; Kaneda, M.; Murai, Y.; Karaushi, H.; Mitsutake, K.; Yamamoto, Y. Effectiveness and Safety of Linezolid Versus Vancomycin, Teicoplanin, or Daptomycin against Methicillin-Resistant *Staphylococcus aureus* Bacteremia: A Systematic Review and Meta-Analysis. *Antibiotics* **2023**, 12 (4), 697.
- (8) Miyamoto, F.; Naoki, H.; Naya, Y.; Nakanishi, K. Study of the secretion from a scale insect (*Ceroplastes ceriferus*) diterpenoids and sesterterpenoids. *Tetrahedron* **1980**, 36 (24), 3481–3487.
- (9) Qi, W.; Zhao, J.; Wei, W.; Gao, K.; Yue, J. Quorumolides A–C, Three Cembranoids from *Euphorbia antiquorum*. *J. Org. Chem.* **2018**, 83 (2), 1041–1045.
- (10) Bu, Q.; Yang, M.; Yan, X.; Yao, L.; Guo, Y.; Liang, L. New flexible cembrane-type macrocyclic diterpenes as TNF- α inhibitors from the South China Sea soft coral *Sarcophyton mililatensis*. *Int. J. Biol. Macromol.* **2022**, 222, 880–886.
- (11) Mohamed, T. A.; Elshamy, A. I.; Abd El-Razek, M. H.; Abdel-Tawab, A. M.; Ali, S. K.; Aboelmagd, M.; Suenaga, M.; Pare, P. W.; Umeyama, A.; Hegazy, M. E. F. *Sarcoconvolutums*, F. and G.

Polyoxygenated Cembrane-Type Diterpenoids from *Sarcophyton convolutum*, a Red Sea Soft Coral. *Molecules* **2022**, *27* (18), 5835.

- (12) Chen, Y. G.; Li, D. S.; Ling, Y.; Liu, Y. C.; Zuo, Z. L.; Gan, L. S.; Luo, S. H.; Hua, J.; Chen, D. Y.; Xu, F.; Li, M.; Guo, K.; Liu, Y.; Gershenzon, J.; Li, S. H. A Cryptic Plant Terpene Cyclase Producing Unconventional 18-and 14-Membered Macrocyclic C₂₅ and C₂₀ Terpenoids with Immunosuppressive Activity. *Angew. Chem., Int. Ed.* **2021**, *60* (48), 25468–25476.
- (13) Luo, P.; Huang, J.; Lv, J.; Wang, G.; Hu, D.; Gao, H. Biosynthesis of fungal terpenoids. *Nat. Prod. Rep.* **2024**, *41* (5), 748–783.
- (14) Yin, Z.; Dickschat, J. S. Engineering fungal terpene biosynthesis. *Nat. Prod. Rep.* **2023**, *40* (1), 28–45.
- (15) Chen, S.; Cai, R.; Liu, Z.; Cui, H.; She, Z. Secondary metabolites from mangrove-associated fungi: source, chemistry and bioactivities. *Nat. Prod. Rep.* **2022**, *39* (3), 560–595.
- (16) Shi, Y.; Ji, M.; Dong, J.; Shi, D.; Wang, Y.; Liu, L.; Feng, S.; Liu, L. New bioactive secondary metabolites from fungi: 2023. *Mycology* **2024**, *15* (3), 283–321.
- (17) Toyomasu, T.; Tsukahara, M.; Kaneko, A.; Niida, R.; Mitsunashi, W.; Dai, T.; Kato, N.; Sassa, T. Fusicoccins are biosynthesized by an unusual chimera diterpene synthase in fungi. *Proc. Natl. Acad. Sci. USA* **2007**, *104* (9), 3084–3088.
- (18) Mitsunashi, T.; Abe, I. Chimeric Terpene Synthases Possessing both Terpene Cyclization and Prenyltransfer Activities. *ChemBioChem* **2018**, *19* (11), 1106–1114.
- (19) Zhang, P.; Qi, J.; Duan, Y.; Gao, J.; Liu, C. Research Progress on Fungal Sesterterpenoids Biosynthesis. *J. Fungi* **2022**, *8* (10), 1080.
- (20) Tao, H.; Lauterbach, L.; Bian, G. K.; Chen, R.; Hou, A. W.; Mori, T.; Cheng, S.; Hu, B.; Lu, L.; Mu, X.; Li, M.; Adachi, N.; Kawasaki, M.; Moriya, T.; Senda, T.; Wang, X. H.; Deng, Z. X.; Abe, I.; Dickschat, J. S.; Liu, T. G. Discovery of non-squalene triterpenes. *Nature* **2022**, *606* (7913), 414–419.
- (21) Chiba, R.; Minami, A.; Gomi, K.; Oikawa, H. Identification of Ophiobolin F Synthase by a Genome Mining Approach: A Sesterterpene Synthase from *Aspergillus clavatus*. *Org. Lett.* **2013**, *15* (3), 594–597.
- (22) Jiang, L.; Zhang, X.; Sato, Y.; Zhu, G.; Minami, A.; Zhang, W.; Ozaki, T.; Zhu, B.; Wang, Z.; Wang, X.; Lv, K.; Zhang, J.; Wang, Y.; Gao, S.; Liu, C.; Hsiang, T.; Zhang, L.; Oikawa, H.; Liu, X. Genome-Based Discovery of Enantiomeric Pentacyclic Sesterterpenes Catalyzed by Fungal Bifunctional Terpene Synthases. *Org. Lett.* **2021**, *23* (12), 4645–4650.
- (23) Wang, M. X.; Carver, J. J.; Phelan, V. V.; Sanchez, L. M.; Garg, N.; Peng, Y.; Nguyen, D. D.; Watrous, J.; Kapon, C. A.; Luzzatto-Knaan, T.; Porto, C.; et al. Sharing and community curation of mass spectrometry data with Global Natural Products Social Molecular Networking. *Nat. Biotechnol.* **2016**, *34* (8), 828–837.
- (24) Nothias, L. F.; Petras, D.; Schmid, R.; Dührkop, K.; Rainer, J.; Sarvepalli, A.; Protasyuk, I.; Ernst, M.; Tsugawa, H.; Fleischauer, M.; et al. Feature-based molecular networking in the GNPS analysis environment. *Nat. Methods* **2020**, *17* (9), 905–908.
- (25) Jiang, L.; Yang, H.; Zhang, X.; Li, X.; Lv, K.; Zhang, W.; Zhu, G.; Liu, C.; Wang, Y.; Hsiang, T.; Zhang, L.; Liu, X. Schultriene and nigtetraene: two sesterterpenes characterized from pathogenetic fungi via genome mining approach. *Appl. Microbiol. Biotechnol.* **2022**, *106* (18), 6047–6057.
- (26) Kumar, S.; Stecher, G.; Li, M.; Knyaz, C.; Tamura, K.; Mega, X. MEGA X: Molecular Evolutionary Genetics Analysis across Computing Platforms. *Mol. Biol. Evol.* **2018**, *35* (6), 1547–1549.
- (27) Jin, F. J.; Maruyama, J.; Juvvadi, P. R.; Arioka, M.; Kitamoto, K. Development of a novel quadruple auxotrophic host transformation system by argB gene disruption using adeA gene and exploiting adenine auxotrophy in *Aspergillus oryzae*. *FEMS Microbiol. Lett.* **2004**, *239* (1), 79–85.
- (28) Oikawa, H. Reconstitution of biosynthetic machinery of fungal natural products in heterologous hosts. *Biosci. Biotechnol. Biochem.* **2020**, *84* (3), 433–444.
- (29) Chambers, M. C.; Maclean, B.; Burke, R.; Amodei, D.; Ruderman, D. L.; Neumann, S.; Gatto, L.; Fischer, B.; Pratt, B.; Egertson, J.; Hoff, K.; et al. A cross-platform toolkit for mass spectrometry and proteomics. *Nat. Biotechnol.* **2012**, *30* (10), 918–920.
- (30) Pluskal, T.; Castillo, S.; Villar-Briones, A.; Orešič, M. MZmine 2: Modular framework for processing, visualizing, and analyzing mass spectrometry-based molecular profile data. *BMC Bioinf.* **2010**, *11*, 395.
- (31) Gerards, M.; Snatzke, G. Circular dichroism, XCD determination of the absolute configuration of alcohols, olefins, epoxides, and ethers from the CD of their “in situ” complexes with [Rh₂(O₂CCF₃)₄]. *Tetrahedron: Asym.* **1990**, *1* (4), 221–236.
- (32) Frelek, J.; Szczepek, W. J. [Rh₂(OCOCF₃)₄] as an auxiliary chromophore in chiroptical studies on steroidal alcohols. *Tetrahedron: Asym.* **1999**, *10* (8), 1507–1520.
- (33) Frisch, M. J.; Trucks, G. W.; Schlegel, H. B.; Scuseria, G. E.; Robb, M. A.; Cheeseman, J. R.; Scalmani, G.; Barone, V.; Mennucci, B.; Petersson, G. A. *Gaussian 09, Revision A.1*. 2009.
- (34) Jiang, L.; Lv, K.; Zhu, G.; Lin, Z.; Zhang, X.; Xing, C.; Yang, H.; Zhang, W.; Wang, Z.; Liu, C.; Qu, X.; Hsiang, T.; Zhang, L.; Liu, X. Norditerpenoids biosynthesized by varied diene synthase-associated P450 machinery along with modifications by the host cell *Aspergillus oryzae*. *Synth. Syst. Biotechnol.* **2022**, *7* (4), 1142–1147.
- (35) Ceriotti, F.; Zakowski, J.; Sine, H.; Altaie, S.; Horowitz, G.; Pesce, A. J.; Boyd, J.; Horn, P.; Gard, U.; Horowitz, G.; The Clinical and Laboratory Standards Institute (CLSI), 2012.
- (36) Yu, J.; Guo, H.; Zhang, J.; Hu, J.; He, H.; Chen, C.; Yang, N.; Yang, F.; Lin, Z.; Dai, H.; Ouyang, L.; Liu, C.; Lei, X.; Zhang, L.; Zhu, G.; Song, F. Chrysomycins Anti-Tuberculosis C-Glycoside Polyketides from *Streptomyces* sp. MS751. *Mar. Drugs* **2024**, *22* (6), 259.
- (37) Yang, G. X.; Ge, S. L.; Wu, Y.; Huang, J.; Li, S. L.; Wang, R.; Ma, L. Design, synthesis and biological evaluation of 3-piperazine-carboxylate sarsapogenin derivatives as potential multifunctional anti-Alzheimer agents. *Eur. J. Med. Chem.* **2018**, *156*, 206–215.
- (38) Wu, J. T.; Lv, S. M.; Lu, C. H.; Gong, J.; An, J. B. Effect of 3,3'-Biisofraxidin on Apoptosis of Human Gastric Cancer BGC-823 Cells. *Trop. J. Pharm. Res.* **2015**, *14* (10), 1803–1811.
- (39) Al-Harrasi, A.; Avula, S. K.; Csuk, R.; Das, B. Cembranoids from *Boswellia* species. *Phytochemistry* **2021**, *191*, 112897.
- (40) Zhang, N.; Xu, W.; Yan, Y.; Chen, M.; Li, H.; Chen, L. Cembrane diterpenoids: Chemistry and pharmacological activities. *Phytochemistry* **2023**, *212*, 113703.
- (41) Minami, A.; Ozaki, T.; Liu, C.; Oikawa, H. Cyclopentane-forming di/sesterterpene synthases: widely distributed enzymes in bacteria, fungi, and plants. *Nat. Prod. Rep.* **2018**, *35* (12), 1330–1346.
- (42) Chen, Y. G.; Li, D. S.; Ling, Y.; Liu, Y. C.; Zuo, Z. L.; Gan, L. S.; Luo, S. H.; Hua, J.; Chen, D. Y.; Xu, F.; Li, M.; Guo, K.; Liu, Y.; Gershenzon, J.; Li, S. H. A Cryptic Plant Terpene Cyclase Producing Unconventional 18-and 14-Membered Macrocyclic C-25 and C-20 Terpenoids with Immunosuppressive Activity. *Angew. Chem., Int. Ed.* **2021**, *60* (48), 25468–25476.
- (43) Engels, B.; Heinig, U.; Grothe, T.; Stadler, M.; Jennewein, S. Cloning and Characterization of an *Armillaria gallica* cDNA Encoding Protoilludene Synthase, Which Catalyzes the First Committed Step in the Synthesis of Antimicrobial Melleolides. *J. Biol. Chem.* **2011**, *286* (9), 6871–6878.
- (44) Sipos, G.; Prasanna, A. N.; Walter, M. C.; O'Connor, E.; Balint, B.; Krizsan, K.; Kiss, B.; Hess, J.; Varga, T.; Slot, J.; Riley, R.; Boka, B.; Rigling, D.; et al. Genome expansion and lineage-specific genetic innovations in the forest pathogenic fungi *Armillaria*. *Nat. Ecol. Evol.* **2017**, *1* (12), 1931–1941.
- (45) Kakule, T. B.; Sardar, D.; Lin, Z. J.; Schmidt, E. W. Two Related Pyrrolidinedione Synthetase Loci in *Fusarium heterosporum* ATCC 74349 Produce Divergent Metabolites. *ACS Chem. Biol.* **2013**, *8* (7), 1549–1557.
- (46) Reeves, C. D.; Hu, Z. H.; Reid, R.; Kealey, J. T. Genes for the biosynthesis of the fungal polyketides hypothemycin from *Hypomyces subiculosus* and radicol from *Pochonia chlamydosporia*. *Appl. Environ. Microbiol.* **2008**, *74* (16), 5121–5129.

- (47) Ohtani, I.; Kusumi, T.; Kashman, Y.; Kakisawa, H. High-field FT NMR application of Mosher's method. The absolute configurations of marine terpenoids. *J. Am. Chem. Soc.* **1991**, *113* (11), 4092–4096.
- (48) Nandhini, P.; Kumar, P.; Mickymaray, S.; Alothaim, A. S.; Somasundaram, J.; Rajan, M. Recent Developments in Methicillin-Resistant *Staphylococcus aureus* (MRSA) Treatment: A Review. *Antibiotics* **2022**, *11* (5), 606.
- (49) Xie, W.; Wang, L.; Luo, D.; Soni, V.; Rosenn, E. H.; Wang, Z. *Mycobacterium smegmatis*, a Promising Vaccine Vector for Preventing TB and Other Diseases: Vaccinomics Insights and Applications. *Vaccines* **2023**, *11* (8), 1302.
- (50) Wallace, R. J.; Nash, D. R.; Tsukamura, M.; Blacklock, Z. M.; Silcox, V. A. Human Disease Due to *Mycobacterium smegmatis*. *J. Infect. Dis.* **1988**, *158* (1), 52–59.
- (51) Röse, L.; Kaufmann, S. H. E.; Däugel, S. Involvement of *Mycobacterium smegmatis* undecaprenyl phosphokinase in biofilm and smegma formation. *Microbes Infect.* **2004**, *6* (11), 965–971.
- (52) Minelli, C.; Mangiaterra, G.; Laudadio, E.; Citterio, B.; Rinaldi, S. Investigation on the Synergy between Membrane Permeabilizing Amphiphilic α -Hydrazido Acids and Commonly Used Antibiotics against Drug-Resistant Bacteria. *Molecules* **2024**, *29* (17), 4078.
- (53) Han, W.; Camesano, T. A. LL37-Derived Fragments Improve the Antibacterial Potential of Penicillin G and Ampicillin against Methicillin-Resistant *Staphylococcus aureus*. *Antibiotics* **2023**, *12* (9), 1398.
- (54) Huang, J. H.; Lv, J. M.; Wang, Q. Z.; Zou, J.; Lu, Y. J.; Wang, Q. L.; Chen, D. N.; Yao, X. S.; Gao, H.; Hu, D. Biosynthesis of an anti-tuberculosis sesterterpenoid asperterpenoid A. *Org. Biomol. Chem.* **2019**, *17* (2), 248–251.
- (55) Godela, A.; Rogacz, D.; Pawłowska, B.; Biczak, R. Natural Neuroinflammatory Modulators: Therapeutic Potential of Fungi-Derived Compounds in Selected Neurodegenerative Diseases. *Molecules* **2025**, *30* (15), 3158.
- (56) de Lima, E. P.; Laurindo, L. F.; Catharin, V. C.; Direito, R.; Tanaka, M.; Jasmin Santos German, I.; Lamas, C. B.; Guiguer, E. L.; Araújo, A. C.; Fiorini, A. M.; Barbalho, S. M. Polyphenols, Alkaloids, and Terpenoids Against Neurodegeneration: Evaluating the Neuroprotective Effects of Phytocompounds Through a Comprehensive Review of the Current Evidence. *Metabolites* **2025**, *15* (2), 124.
- (57) Subedi, L.; Yumnam, S. Terpenoids from *Abies holophylla* Attenuate LPS-Induced Neuroinflammation in Microglial Cells by Suppressing the JNK-Related Signaling Pathway. *Int. J. Mol. Sci.* **2021**, *22* (2), 965.
- (58) Fukaya, M.; Nagamine, S.; Ozaki, T.; Liu, Y.; Ozeki, M.; Matsuyama, T.; Miyamoto, K.; Kawagishi, H.; Uchiyama, M.; Oikawa, H.; Minami, A. Total Biosynthesis of Melleolides from *Basidiomycota* Fungi: Mechanistic Analysis of the Multifunctional GMC Oxidase Mld7. *Angew. Chem., Int. Ed.* **2023**, *135* (44), No. e202308881.
- (59) Kingston, D. G. I. Taxol: The chemistry and structure-activity relationships of a novel anticancer agent. *Trends Biotechnol.* **1994**, *12* (6), 222–227.
- (60) Klayman, D. L. *Qinghaosu* (Artemisinin): an Antimalarial Drug from China. *Science* **1985**, *228* (4703), 1049–1055.
- (61) Cheng, S.; Wen, Z.; Chiou, S.; Hsu, C.; Wang, S.; Dai, C.; Chiang, M.; Duh, C. Durumolides A–E, anti-inflammatory and antibacterial cembranolides from the soft coral *Lobophytum durum*. *Tetrahedron* **2008**, *64* (41), 9698–9704.
- (62) Yan, P.; Deng, Z.; Ofwegen, L. v.; Proksch, P.; Lin, W. Lobophytone, O.-T. new biscebranoids and cembranoid from soft coral *Lobophytum pauciflorum*. *Mar. Drugs* **2010**, *8* (11), 2837–2848.



CAS INSIGHTS™

EXPLORE THE INNOVATIONS SHAPING TOMORROW

Discover the latest scientific research and trends with CAS Insights. Subscribe for email updates on new articles, reports, and webinars at the intersection of science and innovation.

Subscribe today

CAS
A division of the American Chemical Society